J. Membrane Biol. 189, 83–92 (2002)
DOI: 10.1007/s00232-002-1005-9

The Journal of
Membrane
Biology

Syncollin Homo-Oligomers Associate with Lipid Bilayers in the Form of Doughnut-shaped Structures

N.A. Geisse, B. Wäsle, D.E. Saslowsky, R.M. Henderson, J.M. Edwardson
Department of Pharmacology, University of Cambridge, Tennis Court Road, Cambridge CB2 1PD, United Kingdom

Received: 16 February 2002/Revised: 17 May 2002

Abstract. Syncollin is a 16-kDa protein that is associated with the luminal surface of the zymogen granule membrane in the pancreatic acinar cell. Detergent-solubilized, purified syncollin migrates on sucrose density gradients as a large (120-kDa) protein, suggesting that it exists naturally as a homo-oligomer. In this study, we investigated the structure of the syncollin oligomer. Chemical cross-linking of syncollin produced a ladder of bands, the sizes of which are consistent with discrete species from monomers up to hexamers. Electron microscopy of negatively stained syncollin revealed doughnut-shaped structures of outer diameter 10 nm and inner diameter 3 nm. Atomic force microscopy (AFM) of syncollin on mica supports at pH 7.6 showed particles of molecular volume 155 nm^3. Smaller particles were observed either at alkaline pH (11.0), or in the presence of a reducing agent (dithiothreitol), conditions that cause dissociation of the oligomer. AFM imaging of syncollin attached to supported lipid bilayers again revealed doughnut-shaped structures (outer diameter 31 nm, inner diameter 6 nm) protruding 1 nm from the bilayer. Finally, addition of syncollin to liposomes rendered them permeable to the water-soluble fluorescent probe 5(6)-carboxyfluorescein. These results are discussed in relation to the possible physiological role of syncollin.

Key words: Syncollin — Exocrine pancreas — Zymogen granule membrane — Atomic force microscopy — Membrane pore

Correspondence to: J.M. Edwardson, email: jme1000@cam.ac.uk

Introduction

Regulated exocytosis in the pancreatic acinar cell involves the fusion of the membranes of zymogen granules with the apical domain of the plasma membrane (Palade, 1975). Exocytosis is triggered by the release of Ca^{2+} from intracellular stores, which in turn is caused by the action of secretagogues at receptors in the basolateral membrane domain (Kasai, Li & Miyashita, 1993; Thorn et al., 1993). As for most other membrane fusion events (Söllner et al., 1993), exocytotic membrane fusion in the acinar cell is SNARE-dependent (Gaisano et al., 1994, 1996, 1997; Hansen, Antonin & Edwardson, 1999). Nevertheless, despite considerable effort, the particular set of SNAREs involved has not been fully defined. It is known that syntaxin 2, the Q-SNARE present on the apical plasma membrane (Gaisano et al., 1996), is required for granule-plasma membrane fusion, and that syntaxin 3, present on the granule membrane, mediates granule-granule fusion (Hansen et al., 1999). However, synaptobrevin 2, the only R-SNARE so far found on the granule membrane, appears to play only a minor role in exocytotic membrane fusion (Gaisano et al., 1994; Hansen et al., 1999). A search for SNARE binding partners on the granule membrane yielded syncollin, a 16-kDa protein that binds to syntaxin in a Ca^{2+}-sensitive manner (Edwardson, An & Jahn, 1997). Surprisingly, however, it was subsequently found that syncollin exists in tight association with the luminal surface of the membrane of the pancreatic zymogen granule (An et al., 2000), which of course raises doubts about the physiological significance of its ability to bind syntaxin.

Syncollin has a number of unusual biochemical properties. For instance, it resists washing of the zymogen granule membrane with high-salt buffers (e.g., 1 M NaCl), but is removed at high pH (11.0)

(An et al., 2000). At high pH, syncollin migrates on sucrose density gradients as a monomer. When the pH is lowered, syncollin precipitates, and can be solubilized in detergents such as deoxycholate. Under these conditions, syncollin behaves as a large (120-kDa) protein, suggesting that it forms homo-oligomers (An et al., 2000). The association of syncollin with the granule membrane also requires cholesterol: cholesterol depletion using methyl-β-cyclodextrin causes its dissociation, and purified syncollin readily reassociates with liposomes (at pH 5.0, but not at pH 11.0), provided they contain cholesterol (Hodel et al., 2001). Finally, syncollin interacts with GP-2, the major glycoprotein of the granule membrane, and both proteins are recovered in Lubrol-insoluble complexes prepared from the membrane (Kalus et al., 2002), which may indicate that they exist in microdomains ('rafts') in the plane of the membrane (Röper, Corbeil & Huttner, 2000; Schmidt et al., 2001).

In this study, we have used various approaches to probe further the structure of syncollin. Chemical cross-linking has been used to confirm our previous suggestion that syncollin is a homo-oligomer, and to provide clues as to the stoichiometry of this structure. Syncollin has been imaged both by electron microscopy and by atomic force microscopy (AFM) and shown to be doughnut-shaped. Finally, we report that syncollin is able to permeabilize liposomes. In light of these results we discuss the possible physiological role of syncollin.

Materials and Methods

Preparation of Rat Pancreatic Zymogen Granules

Zymogen granules were isolated essentially as described previously (Hodel et al., 2001). All buffers contained a protease inhibitor cocktail (1 mM phenylmethylsulfonyl fluoride and (in μg/ml) 1 pepstatin, 1 antipain, 1 leupeptin, 10 soybean trypsin inhibitor, 17 benzamidine, and 50 bacitracin). Granules were lysed by incubation for 30 min at 4°C in 170 mM NaCl and 200 mM $NaHCO_3$ (pH 7.8; 1:3). Granule membranes were collected by centrifugation at 21,000 × g for 15 min.

Purification of Syncollin

All procedures were carried out at 4°C. Zymogen granule membranes prepared freshly from 5 rats were resuspended in 200 μl of HEPES-buffered saline (50 mM HEPES, pH 7.6, 100 mM NaCl; HBS). KCl was added to a final concentration of 200 mM, and the sample was incubated for 30 min, with shaking. The washed membranes were collected by centrifugation at 21,000 × g for 15 min. The supernatant, containing proteins that had been loosely bound to the granule membranes, was discarded. The membrane pellet was resuspended in 1 ml of 0.1 M Na_2CO_3, and incubated for 30 min, again with shaking. The membranes were pelleted by centrifugation at 21,000 × g for 15 min. The supernatant was recovered and dialyzed overnight against HBS, pH 7.6. The resulting precipitate was collected by centrifugation at 21,000 × g for 15 min. The pellet was dissolved in 100 μl of 0.5% deoxycholate in HBS, pH 7.6. Any insoluble material was pelleted by centrifugation at 21,000 × g for 5 min. The protein concentration of the final sample was typically 20 μg/ml.

SDS-PAGE and Immunoblotting

Proteins were separated by SDS-PAGE and then, where appropriate, electrophoretically transferred to nitrocellulose (Schleicher & Schuell, Dassel, Germany) by semi-dry blotting. Blots were probed with mouse monoclonal anti-syncollin antibody 87.1 (An et al., 2000) at a dilution of 1:1000. Immunoreactive bands were visualized using horseradish peroxidase-conjugated goat anti-mouse secondary antibody (1:1000) and enhanced chemiluminescence (Pierce & Warriner, Chester, United Kingdom). Semi-quantitative analysis of proteins present on Coomassie blue-stained gels was carried out by densitometry using an ImageMaster system (Pharmacia Biotech, St. Albans, United Kingdom).

Chemical Cross-linking of Syncollin

Syncollin (200 ng in HBS, pH 7.6, containing 0.5% deoxycholate), was incubated with the cross-linker bis(sulfosuccinimidyl) suberate (BS^3; 4 mM; Pierce & Warriner) in the absence or presence of dithiothreitol (DTT; 50 mM) for 30 min at 4°C. Cross-linking was terminated by addition of 100 mM Tris, 100 mM glycine, pH 7.5. Pre-quenched BS^3 was used for control incubations. Samples were then analyzed by SDS-PAGE.

Electron Microscopy

Formvar carbon-coated grids were glow-discharged in an Edwards 306 evaporation unit, and used within 24 hr. Grids were floated for 1 min on 10-μl drops of syncollin (20 μg/ml protein in 0.5% deoxycholate/HBS, pH 7.6), or buffer only. Grids were rinsed twice for 5 sec in deionized water, and placed onto a drop of 1% aqueous uranyl acetate for 2 min. Excess stain was blotted onto filter paper, and the grids were allowed to dry for 1 hr. Samples were viewed using a Philips CM100 electron microscope, at 80 kV.

Atomic Force Microscopy

AFM imaging was performed using a Digital Instruments MultiMode atomic force microscope (Digital Instruments, Santa Barbara, CA) controlled by a Nanoscope IIIa controller with an in-line electronics extender module. The microscope was placed on a silicone-gel vibration isolation pad, which was subsequently mounted on an air table. An acoustic hood was placed over the microscope to reduce interference from ambient room sounds. Imaging under fluid was carried out with oxide-sharpened silicon nitride tips (DNP-S; Digital Instruments). The resonant frequencies of the 200-μm long and 20-μm wide cantilever were chosen to be resonance peaks between 6.0–8.5 kHz, with the actual scanning frequency being 10–30% below the maximal response of the chosen peak. Imaging in air was carried out with etched silicon probes (Digital Instruments) tuned between 250–350 kHz. The microscope was engaged with a 0-nm scan size and the automated scanning force/setpoint adjustment system was overridden by tuning the cantilever 50–100 nm above the surface. Images were captured at a 512 × 512 pixel resolution. All samples were adsorbed on freshly-cleaved muscovite mica (Goodfellow, UK), which was glued to a steel disk. Images were processed with the Digital Instruments AFM image analysis software, and most were treated with a zero- or first-order flattening algorithm.

Free syncollin was imaged in air. Briefly, 50 μl of a 0.13 μg/ml solution was deposited onto the mica. After a 10-min incubation,

the sample was rinsed extensively in distilled/deionized water. The sample was dried under nitrogen for 10 min and imaged immediately. Liposome-associated syncollin was imaged under fluid, as described below.

Molecular Volume Calculation

The molecular volume of the protein particles was determined from particle dimensions derived from AFM images. The height and half-height diameters were measured from multiple cross-sections of the same particle, and the molecular volume of each particle was calculated using the following equation, which treats the particle as a spherical cap:

$$V_m = (\pi h/6)(3r^2 + h^2)$$

where h is the particle height and r is the radius at half height (Schneider et al., 1998).

Liposome Preparation and Syncollin Binding

Brain lipids (Avanti Polar Lipids, Alabaster, AL) were supplied in chloroform. The chloroform was evaporated from 2 mg of lipid under a stream of nitrogen, and the lipid was hydrated overnight at 4°C in 500 μl of water. The lipid suspension was sonicated with a probe sonicator (tip amplitude 10 μm, for two bursts of 10 sec) to produce liposomes. An equal volume of either 2-fold concentrated HBS, pH 7.6, or 200 mM Na_2CO_3, pH 11.0, was then added. Purified syncollin (10 μl, 200 ng protein in 0.5% deoxycholate) was added to 1 mg liposomes in a 500 μl volume. (The final detergent concentration was therefore 0.01%). Samples were incubated for 30 min at 4°C, with agitation, and syncollin binding to the liposomes was then analyzed by sucrose density gradient centrifugation.

Sucrose Density Gradient Centrifugation

Samples (500 μl) of liposomes after incubation with syncollin were added to 1.5 ml of 80% sucrose in the appropriate buffer (either HBS, pH 7.6, or 0.1 M Na_2CO_3, pH 11.0). Onto this suspension (now 60% sucrose) was layered 1.5 ml of 50% sucrose in buffer followed by 1.5 ml of buffer alone. The gradient was centrifuged at 140,000 × g for 2 hr at 4°C. Fractions (500 μl) were taken from the top of the gradient and analyzed by SDS-PAGE and immunoblotting.

Production of Supported Lipid Bilayers

Supported lipid bilayers were formed by deposition of a liposome suspension onto mica, followed by incubation for 10–15 minutes. Care was taken to avoid drying the sample during this incubation. After adsorption, samples were gently rinsed with a stream of filtered buffer at the same pH as that of the vesicle preparation, to remove any un-adsorbed vesicles that were still present in the sample. Samples were then imaged in HBS, pH 7.6, containing 3 mM $MgCl_2$, as described above.

Liposome Permeabilization Assay

Protein-free liposomes were prepared as described above, except that overnight hydration of the lipids and sonication occurred in the presence of 80 mM 5(6)-carboxyfluorescein (Sigma, Poole, Dorset). Probe-loaded liposomes were floated on a discontinuous sucrose density gradient in HBS, pH 7.6 to remove free 5(6)-carboxyfluorescein. Liposomes (5 μl) were added to 1 ml of prewarmed (37°C) HBS, pH 7.6 in a thermostatted fluorimeter (Hitachi F-2000), and fluorescence measured (excitation wavelength 490 nm; emission wavelength 520 nm). After a stable baseline signal had been achieved (approximately 1 min), various amounts of syncollin in HBS, pH 7.6, containing 0.5% deoxycholate, were added in a constant volume (2 μl; final detergent concentration 0.001%). The sample was mixed thoroughly and fluorescence was monitored for a further 4 min at 37°C. At the end of the incubation, the total fluorescence was determined after solubilization of the lipids with 0.2% Triton X-100. Fluorescence measured during the incubation was expressed as a percentage of this total value.

Results

The Homo-Oligomeric Structure of Syncollin

Native syncollin was prepared routinely by washing zymogen granule membranes with Na_2CO_3 solution (0.1 M, pH 11.0), and then slowly reducing the pH to 7.6 by dialysis against HBS. Under these conditions, syncollin is selectively precipitated and can be redissolved in 0.5% deoxycholate (An et al., 2000). Fig. 1*A* illustrates the appearance of a typical syncollin sample on a Coomassie blue-stained SDS-polyacrylamide gel. It can be seen that the gel contains a major band running at 16 kDa, a minor band at 34 kDa and three very faint bands between 45 and 66 kDa. We have shown previously by immunoblotting using a rabbit anti-syncollin antibody (Hodel et al., 2001) that the 16-kDa band represents the syncollin monomer, while the 34-kDa band represents a syncollin dimer, that resists heat-treatment of the samples. The fainter bands do not react with anti-syncollin antibodies, and therefore represent contaminants. Densitometric scanning of the gel shown in Fig. 1*A* indicated that the syncollin bands account for >95% of the total protein in the sample.

We used the water-soluble cross-linking reagent BS^3 to reveal the oligomeric nature of syncollin. Following incubation of deoxycholate-solubilized syncollin with BS^3, a ladder of bands was apparent on a syncollin blot, probed with the mouse monoclonal anti-syncollin antibody 87.1 (Fig. 1*B*). The most prominent band was at 16 kDa, which corresponds with the monomer. Five fainter bands were seen, at approximate molecular masses 34 kDa, 48 kDa, 64 kDa, 80 kDa and 100 kDa, which are likely to represent dimers, trimers, and so on, through to hexamers. An additional band of molecular mass 21 kDa was also seen routinely in cross-linked samples, which we cannot presently explain. The fuzziness of the blot towards the top makes it impossible to judge whether there are any additional bands above 100 kDa, although a hexameric structure would be consistent with the behavior of syncollin on sucrose density gradients (An et al., 2000). When the BS^3 was prequenched by incubation with Tris/glycine, only the syncollin monomer was seen, as expected. Note that the syncollin dimer, seen on the Coomassie-stained gel (Fig. 1*A*), and previously using a rabbit polyclonal anti-syncollin antibody (Hodel et al., 2001), was not detected using the mouse monoclonal antibody.

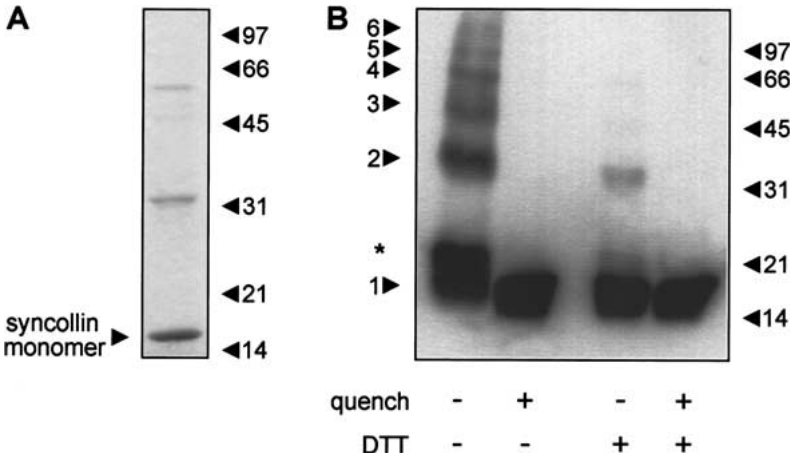

Fig. 1. The homo-oligomeric structure of syncollin, and its stabilization by intramolecular disulfide bonding. (*A*) Purified syncollin (250 ng of protein) in gel sample buffer was heated at 95°C for 5 min and then analyzed by SDS-PAGE and Coomassie blue staining. The position of the syncollin monomer is indicated. The band running at 34 kDa has been shown to react with a rabbit polyclonal anti-syncollin antibody, and likely represents a syncollin dimer; the bands between 45 and 66 kDa are impurities. (*B*) Purified syncollin (200 ng protein in 0.5% deoxycholate) was incubated with active or prequenched BS^3, either in the absence or presence of DTT (50 mM), for 30 min at 4°C. Active BS^3 was quenched by addition of 100 mM Tris, 100 mM glycine, and the protein was analyzed by SDS-PAGE and immunoblotting, using anti-syncollin antibody 87.1. The positions of molecular mass markers (in kDa) are shown on the right. The positions of the various syncollin structures (monomer to hexamer) are shown on the left. The asterisk indicates an additional unidentified band.

It is known that syncollin has intra-molecular disulfide bonds (An et al., 2000). We therefore investigated the effect of reducing these bonds on the ability of BS^3 to cause cross-linking of the monomers. As shown in Fig. 2*B*, cross-linking carried out in the presence of DTT (50 mM) was very inefficient: the syncollin dimer was faint, and the higher bands described previously were almost invisible. DTT was found to have no effect on the protein cross-linking pattern obtained when detergent extracts of zymogen granule membrane were incubated with BS^3 (*not shown*), indicating that it does not affect the cross-linking reaction itself. Hence, we can conclude that the integrity of the syncollin oligomer depends on the presence of intramolecular disulfide bonds.

Electron Microscopy of Syncollin

Syncollin, dissolved in 0.5% deoxycholate, was allowed to attach to carbon-coated grids, negatively stained and visualized in the electron microscope. As shown in Fig. 2*A*, syncollin appeared as a population of particles, some of which were clearly doughnut-shaped. These particles were absent when an identical detergent solution without syncollin was subjected to the same analysis (*not shown*). A gallery of zoomed images of syncollin particles is shown in Fig. 2*B*. It can be seen that the doughnuts have an outer diameter of approximately 10 nm and an inner diameter of approximately 3 nm.

AFM Imaging of Syncollin on Mica

AFM represents an attractive method for imaging syncollin, since it provides resolution at least comparable with that of electron microscopy, but offers the additional advantage of being able to operate under near-physiological conditions (Ellis et al., 1999a,b). As a first step, syncollin, in HBS, pH 7.6, containing 0.5% deoxycholate, was bound to a mica support, dried down and imaged in air. As shown in Fig. 3*A*, a relatively homogeneous population of particles was seen, usually in association with a film of thickness 0.5 nm, which is likely to be residual detergent (deoxycholate). Previous biochemical experiments had indicated that syncollin breaks down into monomers at high pH (11.0) (An et al., 2000), and also in the presence of the reducing agent, DTT (*see* above). With this in mind, we prepared samples of syncollin bound to mica under these conditions, and imaged them by AFM. As shown in Fig. 3*B*, *C*, the particles observed at pH 11.0 and in the presence of DTT, respectively, were in both cases smaller than those seen at pH 7.6 without DTT (Fig. 3*A*). The dimensions of populations of the particles illustrated in Fig. 3*A–C* were determined, and used to calculate their apparent molecular volumes. Particle diameter was measured at half the maximal height to compensate for the tendency of AFM to overestimate this parameter, because of the geometry of the scanning tip (Lärmer et al., 1997; Ellis et al., 1999a, b; Berge et al., 2000). Histograms of the values obtained are shown in Fig. 3*D*. Median molecular volumes were 155 nm^3 at pH 7.6 ($n = 51$), 29 nm^3 at pH 11.0 ($n = 48$), and 52 nm^3 at pH 7.6 in the presence of DTT ($n = 119$). It is apparent, therefore, that incubation of syncollin either at pH 11.0 or in the presence of DTT causes a substantial reduction in its apparent molecular volume, consistent with previous evidence that the syncollin homo-oligomer dissociates into monomers under these conditions (*see* above, and An et al., 2000).

AFM Imaging of Syncollin in Association with Supported Lipid Bilayers

Syncollin was added to a suspension of brain liposomes in a small volume of detergent solution (0.5%

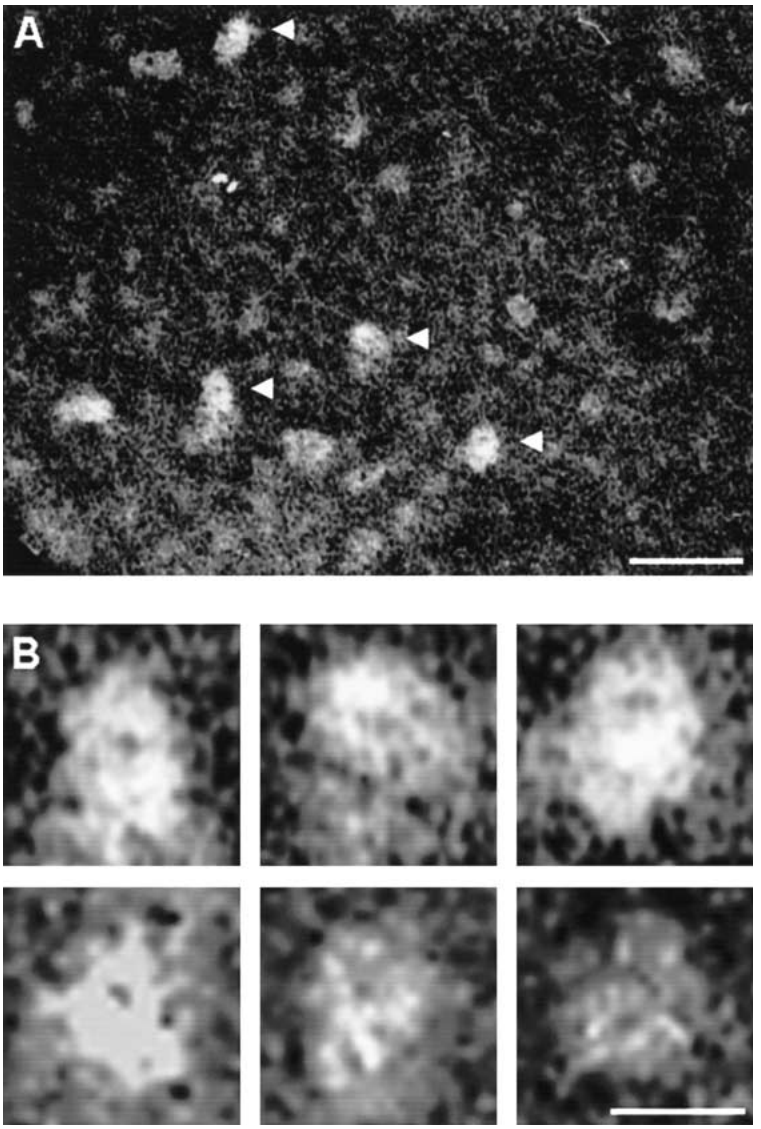

Fig. 2. Electron microscopy of negatively stained syncollin reveals doughnut-shaped structures. Syncollin (10 μl of 20 μg/ml protein in 0.5% deoxycholate/HBS, pH 7.6), was deposited on carbon-coated Formvar grids, and attached protein was negatively stained with uranyl acetate and visualized in the electron microscope. (*A*) Low-magnification electron micrograph, showing a population of doughnut-shaped particles (arrowheads). Bar, 50 nm. (*B*) Gallery of zoomed images, illustrating the doughnut structure of syncollin. Bar, 10 nm.

deoxycholate), followed by incubation at 4°C for 30 min. When the incubation was carried out at pH 7.6, almost all of the syncollin became associated with the liposomes, as judged by its flotation with the lipids on a discontinuous sucrose density gradient (Fig. 4*A*). In contrast, when the incubation was carried out at pH 11.0, no syncollin was detected at the top of the gradient; instead, it remained in the loading zone after centrifugation (Fig. 4*A*). Hence, syncollin binds efficiently to liposomes at pH 7.6, but not at all at pH 11.0. When the suspension of liposomes containing syncollin was harvested from the gradient, and placed onto a mica substrate, some of the liposomes became attached to the mica and collapsed to form supported lipid bilayers. The presence of syncollin on the mica was confirmed by resuspension of the bound material, followed by analysis by SDS-PAGE and immunoblotting, using the mouse monoclonal anti-syncollin antibody 87.1 (Fig. 4*B*).

When syncollin-free liposomes were imaged by AFM under fluid, flat featureless islands were observed on the mica support (Fig. 4*C*). Syncollin-containing liposomes, produced by incubation at pH 7.6 followed by flotation on a sucrose gradient, gave similar islands of bilayer (Fig. 4*D*). Now, however, the bilayers contained populations of particles on their upper surfaces. Determination of the height of the islands (4.5 nm) confirmed that they were indeed lipid bilayers (Sprong, van der Sluijs & van Meer, 2001). When the incubation of syncollin with liposomes was carried out at pH 11.0 (which did not result in association of the protein with the liposomes; Fig. 4*A*), the bilayers were once again featureless (Fig. 4*E*). The fact that syncollin represents >95% of the total protein added to the liposomes (*see* above), and that syncollin present on the mica was detectable by immunoblotting, combined with the observation of particles only under conditions where syncollin is

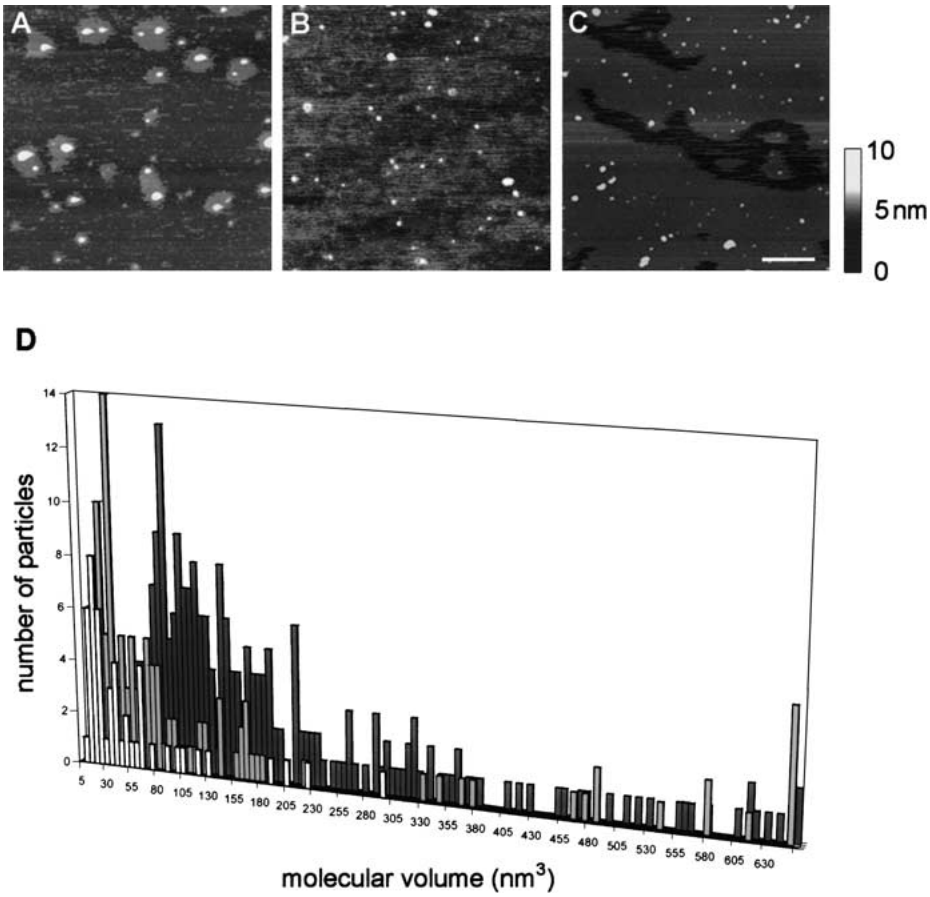

Fig. 3. Syncollin homo-oligomers, visualized by AFM, dissociate at high pH and in a reducing environment. Syncollin was imaged on freshly cleaved mica. Syncollin, in the appropriate buffer containing 0.5% deoxycholate, was allowed to adsorb to the surface. The sample was then washed with water and dried under a stream of nitrogen. Samples were imaged in air, using tapping mode. Syncollin was deposited on the mica in either HBS, pH 7.6 (*A*), Na_2CO_3, pH 11.0 (*B*), or HBS, pH 7.6 containing 1 mM DTT (*C*). A shade-height scale is shown at the right. Bar, 200 nm. (*D*) Histograms showing the distribution of molecular volumes of populations of particles illustrated in *A* (black bars), *B* (white bars) and *C* (gray bars).

known to bind to the liposomes, strongly suggests that the particles imaged represent syncollin molecules.

A higher-magnification image of a supported lipid bilayer containing syncollin is shown in Fig. 5*A*. At this magnification, the particles attached to the bilayer appear as doughnut-shaped structures. A gallery of images of these structures is shown in Fig. 5*B*. The outer diameter of the doughnuts at half-height is 31 ± 7 nm (mean ± SD; $n = 9$), and the inner diameter is 6 ± 3 nm ($n = 9$). Fig. 5*C* shows a 3-dimensional image of an exceptionally well-resolved structure, clearly showing the doughnut shape protruding from the lipid bilayer by approximately 1 nm, and also hinting at a hexameric arrrangement of subunits.

Values quoted by the manufacturers (Digital Instruments) for the radius of an oxide-sharpened AFM tip are in the range 5–40 nm, and values reported previously are 11–23 nm (Laney et al., 1997). It should therefore be difficult to resolve the depression in the syncollin doughnut by AFM. However, resolution of ~1 nm on scattered samples is in fact obtainable, most likely because of variability in the quality of the manufactured tip, as well as the effects of scanning conditions and sample contamination (Czajkowsky & Shao, 1998; Sheng, Czajkowsky & Shao, 1999; Czajkowski, Iwamoto & Shao, 2000). Further, tip radii as small as 1 nm, based on 'blind' reconstruction techniques, are possible on commercially available silicon nitride tips (Sheng et al., 1999).

Syncollin-induced Permeabilization of Liposomes

The close association of syncollin with lipid bilayers, and the doughnut structure observed in these studies, suggests that syncollin might have pore-forming properties. To test this idea directly, we loaded liposomes with the hydrophilic fluorescent probe 5(6)-

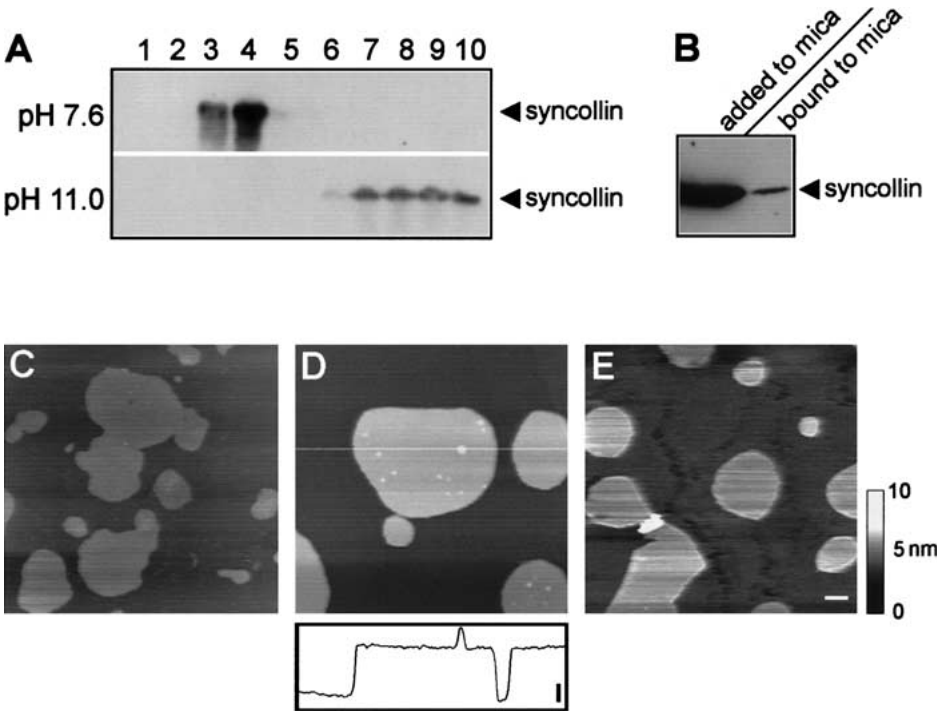

Fig. 4. AFM imaging of syncollin in association with supported lipid bilayers. (*A*) Syncollin was incubated with a suspension of liposomes, either in HBS, pH 7.6, or in Na_2CO_3, pH 11.0, for 30 min at 4°C. Liposomes were then floated on a discontinuous sucrose density gradient. Fractions (1–10) were taken from the top of the gradient and analyzed by SDS-PAGE and immunoblotting, using mouse monoclonal anti-syncollin antibody 87.1. Lipids were recovered predominantly in fractions 3 and 4 (*not shown*). (*B*) Liposome-associated syncollin was harvested from fraction 3 of the sucrose gradient described in *A*, diluted 1:5 and added to mica to form a supported lipid bilayer. Material attached to the mica was resuspended in gel sample buffer and analyzed by SDS-PAGE and immunoblotting, along with a sample of the liposome suspension. Protein-free liposomes (*C*), and liposomes that had been incubated with syncollin either at pH 7.6 (*D*) or pH 11.0 (*E*) were floated on discontinuous sucrose density gradients, as in (*A*). Fraction 3 was harvested from each gradient and used to prepare lipid bilayers on mica supports. AFM imaging was carried out in tapping mode under fluid. A shade-height scale is shown at the right. The section through sample *D*, taken at the position indicated by the line, indicates a bilayer thickness of 4.5 nm. Vertical scale bar, 2 nm; horizontal scale bar, 200 nm.

carboxyfluorescein, at a concentration that caused self-quenching of its fluorescence, and used the relief of this self-quenching caused by its leakage from the liposomes as an index of the ability of syncollin to cause permeabilization. The extent of initial quenching could be assessed by measuring the increase in fluorescence when the lipids were dissolved by addition of the detergent Triton X-100 (0.2%). Of necessity, syncollin had to be added to the sample of loaded liposomes (total volume 1 ml) in a small volume (2 µl) of 0.5% deoxycholate solution, which resulted in a final detergent concentration in the incubation mix of 0.001%. This concentration of detergent caused a small de-quenching signal, indicating a small degree of permeabilization of the liposomes (Fig. 6*A*). When increasing concentrations of syncollin were added to the liposomes in a constant volume of detergent solution, however, increasing extents of time-dependent de-quenching were observed. The largest amount of syncollin used in the experiment illustrated (4 ng) produced 20% of the de-quenching caused by addition of Triton X-100. Two control experiments were carried out to confirm that it was in fact the syncollin that was bringing about the permeabilization of the liposomes. First, syncollin was heated at 100°C for 5 min before addition. As shown in Fig. 6*B*, no significant de-quenching now occurred above that produced by detergent alone. Second, the experiment was carried out at pH 11.0, which does not result in syncollin binding to liposomes (*see* above). Once again, syncollin addition had no effect (Fig. 6*C*). Hence, the association of syncollin with liposomes at pH 7.6 does indeed cause their permeabilization.

Discussion

In this study, we have confirmed that under physiological conditions syncollin exists as a homo-oligomer, most likely a hexamer. Further, through the use of two independent imaging techniques, we have shown that this oligomer forms a doughnut-shaped structure, both when bound to a solid support, and in

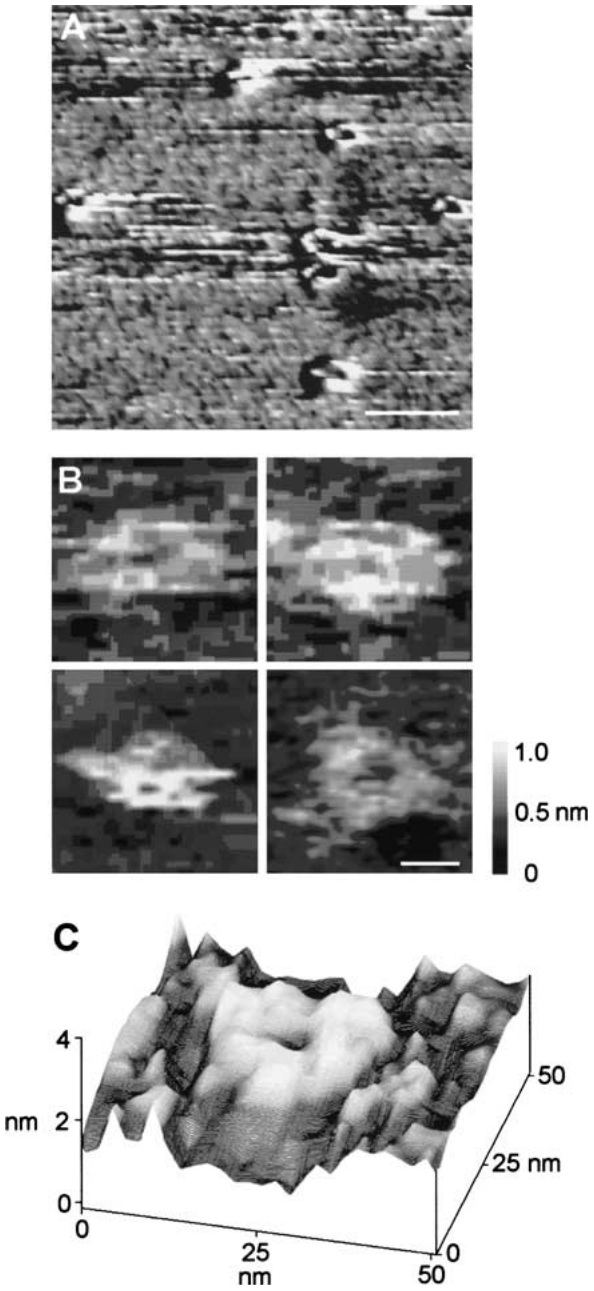

Fig. 5. Lipid-associated syncollin adopts a doughnut-shaped structure. (*A*) Three-dimensional view of a population of syncollin molecules associated with a supported lipid bilayer, imaged in tapping mode under fluid. Scale bar, 50 nm. (*B*) Gallery of higher-magnification images of syncollin. A shade-height scale is shown at the right. Scale bar, 10 nm. (*C*) High-magnification, three-dimensional view of a bilayer-associated syncollin molecule, illustrating the doughnut structure of the protein.

association with a lipid bilayer, the state in which it naturally exists. The apparent diameter of the doughnut observed when syncollin was imaged bound to lipid bilayers was considerably larger than that estimated for syncollin on a solid support. This difference might reflect a real difference in the structure of the molecule under the two conditions, although factors arising from the imaging procedures themselves might also be involved. For instance, electron microscopy necessitates dehydration of the syncollin, whereas size measurement by AFM is complicated by convolution caused by the geometry of the AFM scanning tip. In addition to these structural data, we also present evidence that the pore-like structure of syncollin has a functional correlate in its ability to permeabilize liposomes.

Interestingly, it was shown several years ago, using freeze-fracture electron microscopy, that doughnut-shaped particles are present in the zymogen granule membrane (Cabana et al., 1987). Two populations of these particles were observed: one of outer diameter 15 nm and inner diameter 5 nm, and another of outer diameter 13 nm. The latter type of particle was the more common, accounting for 26% of the particles observed in the luminal leaflet of the membrane, but only 8% of the particles in the cytoplasmic leaflet, consistent with the association of protein with the membrane from the luminal side. These particles have dimensions very similar to those determined here for isolated syncollin. Furthermore, it has been shown that the distribution of cholesterol between the two leaflets of the granule membrane changes from being predominantly cytoplasmic to predominantly luminal as the granule matures (Orci et al., 1980). Since syncollin binds to lipid bilayers in a cholesterol-dependent manner (Hodel et al., 2001), this change would favor the attachment of syncollin to the membrane of the mature granule.

The function of the doughnut-shaped particles seen previously in the granule membrane is still unclear. It has been reported that isolated zymogen granules are leaky to proteins (Goncz & Rothman, 1992), and evidence has been presented that the relative permeability of the membrane to digestive enzymes of different molecular masses is consistent with the presence of a pore of effective diameter 5 nm (Goncz & Rothman, 1995). Furthermore, it has been argued that the ability of proteins to cross the granule membrane is critical to the normal process of secretion in the acinar cell (Isenman, Liebow & Rothman, 1995).

The ability to permeabilize liposomes represents another property that connects syncollin with the pore-like structures seen previously. The nature of the permeabilization brought about by syncollin clearly requires further investigation. 5(6)-carboxyfluorescein has a molecular mass of 376 Da, suggesting that syncollin allows the passage of reasonably large species. In the future, the use of a probe such as fluorescently-labeled dextran, which is available in a variety of sizes, might help determine the size cut-off of the pore/lesion induced by syncollin. An investigation of the ability of syncollin to induce channel activity in lipid bilayers is probably also worthwhile.

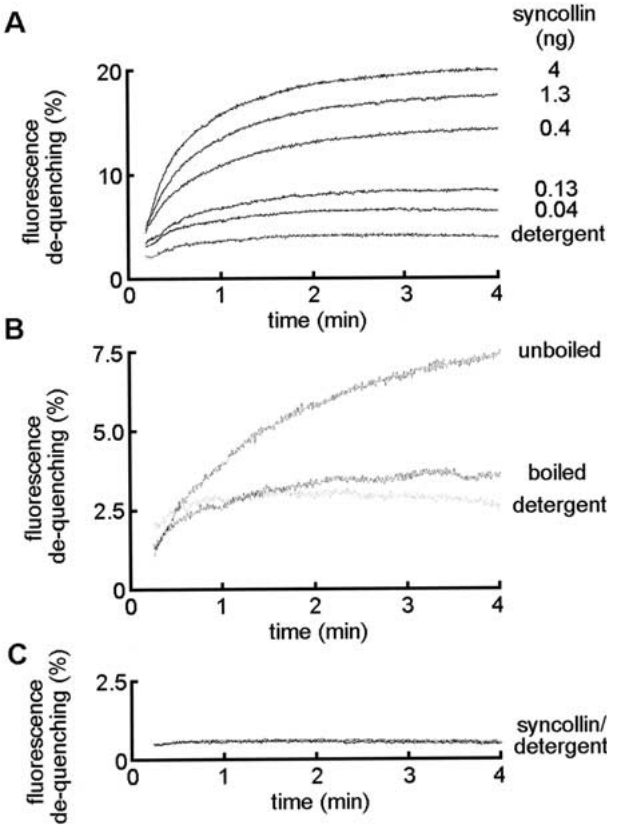

Fig. 6. Syncollin permeabilizes liposomes. Protein-free liposomes were loaded with 5(6)-carboxyfluorescein at a concentration (80 mM) that resulted in self-quenching of its fluorescence. Permeabilization of the liposomes was monitored through the relief of this self-quenching caused by carboxyfluorescein leakage. Fluorescence was measured at 37°C at an excitation wavelength 490 nm and an emission wavelength of 520 nm. Fluorescence de-quenching during the incubation was expressed as a percentage of the total value determined after solubilization of the lipids with 0.2% Triton X-100. (*A*) Concentration- and time-dependent de-quenching caused by syncollin. (*B*) Effect of boiling on the ability of syncollin (4 ng) to cause de-quenching. (*C*) Lack of effect of syncollin at pH 11.0.

This type of study would allow us to distinguish between genuine channel-forming activity and a membrane destabilization of the type shown recently to be caused by pro-apoptotic cleavage products of the protein Bcl-x_L (Basañez et al., 2001).

Although there is now considerable information about the biochemical properties of syncollin, its physiological role is still not understood. Because of the location of syncollin on the inside of the zymogen granule (An et al., 2000; Hodel et al., 2001), its ability to bind in vitro to syntaxin 2, the Q-SNARE known to be present in the apical domain of the plasma membrane in acinar cells (Gaisano et al., 1996; Hansen et al., 1999), might not be functionally significant. Of course, if it is able under some circumstances to form pores that span the granule membrane, it might indeed be able to interact with syntaxin 2 in the acinar cell. An intriguing possibility is that syncollin interacts with syntaxin 2 at the point at which the granule 'docks' with the apical plasma membrane, and that the complex formed goes on to create a fusion pore. This possibility remains to be tested. The expression of syncollin is known to be modulated by feeding behavior (Tan & Hooi, 2000), suggesting that it does have a role in the secretion of digestive enzymes. Surprisingly, a syncollin 'knockout' mouse has a mild phenotype, which indicates an involvement in zymogen granule biogenesis rather than directly in secretion (Antonin et al., 2002). However, there might be redundancy in the system, with another protein being able to replace, at least to some extent, the function of syncollin in the knockout mouse. The presence of two types of pore-like structures in the granule membrane (Cabana et al., 1987) lends support to this idea. The ability of syncollin to interact with GP-2, which appears to be involved in the adhesion of the intra-granular protein matrix to the granule membrane, might also indicate a role upstream of the final exocytotic membrane fusion event (Kalus et al., 2002). We suggest that the structural information presented here provides a context within which experiments aimed at elucidating the physiological function of syncollin can be designed.

We thank Dr. J. Skepper (Multi-Imaging Laboratory, Department of Anatomy, University of Cambridge, United Kingdom) for expert assistance with the electron microscopy. This work was supported by Project Grant 063920 from the Wellcome Trust (to J.M.E.). N.A.G. is supported by the Cambridge Overseas Trust. D.E.S. is supported by the Biotechnology and Biological Sciences Research Council.

References

An, S.J., Hansen, N.J., Hodel, A., Jahn, R., Edwardson, J.M. 2000. Analysis of the association of syncollin with the membrane of the pancreatic zymogen granule. *J. Biol. Chem.* **275:**11306–11311

Antonin, W., Wagner, M., Riedel, D., Brose, N., Jahn, R. 2002. Loss of the zymogen granule protein syncollin affects pancreatic protein synthesis and transport but not secretion. *Mol. Cell. Biol.* **22:**1545–1554

Basañez, G., Zhang, J., Chau, B.N., Maksaev, G.I., Frolov, V.A., Brandt, T.A., Burch, J., Hardwick, J.M., Zimmerberg, J. 2001. Pro-apoptotic cleavage products of Bcl-x_L form cytochrome c-conducting pores in pure lipid membranes. *J. Biol. Chem.* **276:**31083–31091

Berge, T., Ellis, D.J., Dryden, D.T.F., Edwardson, J.M., Henderson, R.M. 2000. Translocation-independent dimerization of the *Eco*KI endonuclease visualized by atomic force microscopy. *Biophys. J.* **79:**479–484

Cabana, C., Magny, P., Nadeau, D., Grondin, G., Beaudoin, A. 1987. Freeze-fracture study of the zymogen granule membrane of pancreas: two novel types of intramembrane particles. *Eur. J. Cell Biol.* **45:**246–255

Czajkowsky, D.M., Iwamoto, H., Shao Z. 2000. Atomic force microscopy in structural biology: from the subcellular to the submolecular. *J. Electron Microsc.* **49:**395–406

Czajkowsky, D.M., Shao, Z. 1998. Submolecular resolution of single macromolecules with atomic force microscopy. *FEBS Lett*. **430:**51–54

Edwardson, J.M., An, S., Jahn, R. 1997. The secretory granule protein syncollin binds to syntaxin in a Ca^{2+}-sensitive manner. *Cell* **90:**325–333

Ellis, D.J., Berge, T., Edwardson, J.M., Henderson, R.M. 1999a. Investigation of protein partnerships using atomic force microscopy. *Microsc. Res. Tech*. **44:**368–377

Ellis, D.J., Dryden, D.T.F., Berge, T., Edwardson, J.M., Henderson, R.M. 1999b. Direct observation of DNA translocation and cleavage by atomic force microscopy. *Nature Struct. Biol*. **6:**15–17

Gaisano, H.Y., Ghai, M., Malkus P.N., Sheu L., Bouquillon, A., Bennett, M.K., Trimble, W.S. 1996. Distinct cellular locations of the syntaxin family of proteins in rat pancreatic acinar cells. *Mol. Biol. Cell*. **7:**2019–2027

Gaisano, H.Y., Sheu, L., Foskett, J.K., Trimble, W.S. 1994. Tetanus toxin light chain cleaves a vesicle-associated membrane protein (VAMP) isofom 2 in rat pancreatic zymogen granules and inhibits enzyme secretion. *J. Biol. Chem*. **269:**17062–17066

Gaisano, H.Y., Sheu, L., Wong, P.P.C., Klip, A., Trimble, W.S. 1997. SNAP-23 is located in the basolateral membrane of rat pancreatic acinar cells. *FEBS Lett*. **414:**298–302

Goncz, K.K., Rothman, S.S. 1992. Protein flux across the membrane of single secretion granules. *Biochim. Biophys. Acta* **1109:**7–16

Goncz, K.K., Rothman, S.S. 1995. A trans-membrane pore can account for movement across zymogen granule membranes. *Biochim. Biophys. Acta* **1238:**91–93

Hansen, N.J., Antonin, W., Edwardson, J.M. 1999. Identification of SNAREs involved in regulated exocytosis in the exocrine pancreas. *J. Biol. Chem*. **274:**22871–22876

Hodel, A., An, S.J., Hansen, N.J., Lawrence, J., Wäsle, B., Schrader, M., Edwardson, J.M. 2001. Cholesterol-dependent interaction of syncollin with the membrane of the pancreatic zymogen granule. *Biochem. J*. **356:**843–850

Isenman, L., Liebow, C., Rothman, S. 1995. Transport of proteins across membranes — a paradigm in transition. *Biochim. Biophys. Acta* **1241:**341–370

Kalus, L., Hodel, A., Koch, A., Kleene, R., Edwardson, J.M., Schrader, M. 2002. Interaction of syncollin with GP-2, the major membrane protein of pancreatic zymogen granules, and association with lipid microdomains. *Biochem. J*. **362:**433–442

Kasai, H., Li, Y.X., Miyashita, Y. 1993. Subcellular distribution of Ca^{2+} release channels underlying Ca^{2+} waves and oscillations in exocrine pancreas. *Cell* **74:**669–677

Laney, D.E., Garcia, R.A., Parsons, S.M., Hansma, H.G. 1997. Changes in the elastic properties of cholinergic synaptic vesicles as measured by atomic force microscopy. *Biophys. J*. **72:**806–813

Lärmer, J., Schneider, S.W., Danker, T., Schwab, A., Oberleithner, H. 1997. Imaging excised apical plasma membrane patches of MDCK cells in physiological conditions with atomic force microscopy. *Pfluegers Arch*. **434:**254–260

Orci, L., Miller, R.G., Montesano R., Perrelet, A., Amherdt, M., Vassalli, P. 1980. Opposite polarity of filipin-induced deformations in the membrane of condensing vacuoles and zymogen granules. *Science* **210:**1019–1021

Palade, G.E. 1975. Intracellular aspects of protein synthesis. *Science* **189:**347–358

Röper, K., Corbeil, D., Huttner, W.B. 2000. Retention of prominin in microvilli reveals distinct cholesterol-based lipid microdomains in the apical plasma membrane. *Nature Cell Biol*. **2:**582–592

Schmidt, K., Schrader, M., Kern, H.F., Kleene, R. 2001. Regulated apical secretion of zymogens in rat pancreas. *J. Biol. Chem*. **276:**14315–14323

Schneider, S.W., Lärmer, J., Henderson, R.M., Oberleithner, H. 1998. Molecular weights of individual proteins correlate with molecular volumes measured by atomic force microscopy. *Pfluegers Arch*. **435:**362–367

Sheng, S., Czajkowsky, D.M., Shao, Z. 1999. AFM tips: how sharp are they? *J. Microsc*. **196:**1–5

Söllner, T.H., Whiteheart, S.H., Brunner, M., Erdjument-Bromage, H., Geromanos, S., Tempst, P., Rothman, J.E. 1993. SNAP receptors implicated in vesicle targeting and fusion. *Nature* **362:**318–324

Sprong, H., van der Sluijs, P., van Meer, G. 2001. How proteins move lipids and lipids move proteins. *Nature Reviews, Mol. Cell Biol*. **2:**504–513

Tan, S., Hooi, S.C. 2000. Syncollin is differentially expressed in rat proximal small intestine and regulated by feeding behaviour. *Am. J. Physiol*. **278:**G308–320

Thorn, P., Lawrie, A.M., Smith, P.M., Gallacher, D.V., Petersen, O.H. 1993. Local and global cytosolic Ca^{2+} oscillations in exocrine cells evoked by agonist and inositol trisphosphate. *Cell* **74:**661–668